ACS APPLIED MATERIALS & INTERFACES

Research Article

www.acsami.org

Color-Tunable Luminescence of Organoclay-Based Hybrid Materials Showing Potential Applications in White LED and Thermosensors

Tianren Wang, Peng Li, and Huanrong Li*

School of Chemical Engineering and Technology, Hebei University of Technology, Tianjin 300130, China

Supporting Information

ABSTRACT: Hybrid composites with great potential for white light LED and temperature sensing obtained through a simple, low cost, and environmental benign way is highly desirable and remains a challengeable task. Herein we present luminescent hybrid composites both in the form of powder and transparent film by simply mixing organic sensitizer, aminoclay (AC), and lanthanide (Ln^{3+}) in aqueous solution, the emission color of which can be fine-tuned by changing various parameters such as the molar ratio of Eu^{3+} to Tb^{3+}, excitation wavelength, and the temperature. White lights with satisfied color coordinates have been achieved. The emission intensity ratio of $^5D_4 \rightarrow {}^7F_5$ transition (Tb^{3+}) to $^5D_0 \rightarrow {}^7F_2$ transition (Eu^{3+}) of the composite containing both Eu^{3+} and Tb^{3+} can be linearly related to temperature in the range from 78 K to 288 K. These characteristics make the composites suitable for optoelectronic devices such as thermosensors and white light LED.

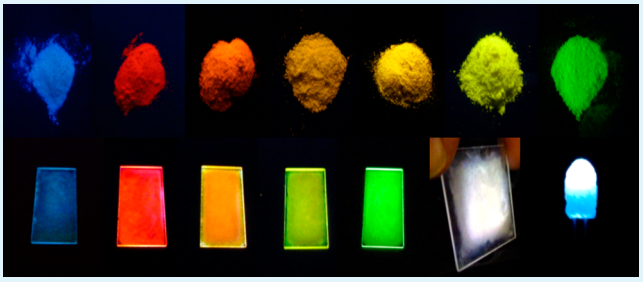

KEYWORDS: *hybrid materials, lanthanide, white light, luminescent thermometer, aminoclay*

1. INTRODUCTION

White-light-emitting materials have gained intense attention in recent years due to their widespread applications in optoelectronic devices such as full color displays and the back-light of portable display devices.[1] In principle, an ideal white-light-emitting system should consist of three primary colors (RGB: red, green, and blue) in desired intensities and cover the visible wavelength range from 380 to 750 nm, which are typically composed of multiple cooperating components or just a single multifunctional emitter.[2−4] This largely relies on the fine control of energy transfer process within or between the components possibly through the proper molecular design and supramolecular organization of various components.[5,6] The organization of organic chromophores within the amino moiety functionalized organoclay[7−9] has been employed to realize processable white-light-emitting materials resulting from the energy transfer between chromophores governed by the organoclay.[10−12]

The application of lanthanide-containing materials in white-light generation has attracted considerable attention due to their unique optical features such as sharp emission bands, large Stokes shift, long lifetime, and tunable emission.[13−19] White-light emission has been produced in an elegantly designed europium(III) complex in which only partial energy transfer from sensitizing fluorophore to Eu^{3+} ions occurs.[20] Duan and co-workers reported tunable emission of three primary colors (red, green, and blue) and white light through the combination of an Eu^{3+} complexes exhibiting red light and an organic ligand consisting of a blue-emitting coumarin fluorophore and a green-emitting Rhodamine 6G fluorophore.[21] Nevertheless, time-consuming and high cost as a result of the multistep synthesis and purifying of ligands constitute the major challenges for the generation of white light to realize their applications in electro-optic devices. Furthermore, drawbacks such as low thermal and photochemical stability and poor mechanical properties as well as inferior processability exhibited by these complexes also severely limit their full exploitation in building devices.[18,19,22−24] The assembly of various trivalent lanthanide ions (Ln^{3+}) and organic sensitizer within inorganic scaffold leads to luminescent hybrid materials with improved stability and bettered luminescence output.[25,26] Multicolored photoluminescence as well as white-light emission were occasionally observed in some of this kind of materials due to the partial energy transfer from sensitizer to Ln^{3+} ions; the organic sensitizer can serve as blue components in addition to being a photosensitizer as a result of the partial energy transfer.[27] However, the generation of white light in such a kind of hybrid materials is fully unexploited since the control of energy transfer to multicomponents is extremely difficult due to the sensitivity of luminescence systems to the chemical environment,[28,29] and only several reports are available.[6,27] For instance, Wada reported the fine-tuning of emission color and white light in NaX zeolite with sensitizer, Eu^{3+} and Tb^{3+} encapsulated within the cavities. A white color was only observed at 77 K, unfortunately.[6] Also inserting organic sensitizers within zeolite cavities has to be done under vigorous

Received: May 9, 2014
Accepted: June 26, 2014
Published: June 26, 2014

 © 2014 American Chemical Society

Scheme 1. Preparation of AC-BTC-Ln Hydrogel[a]

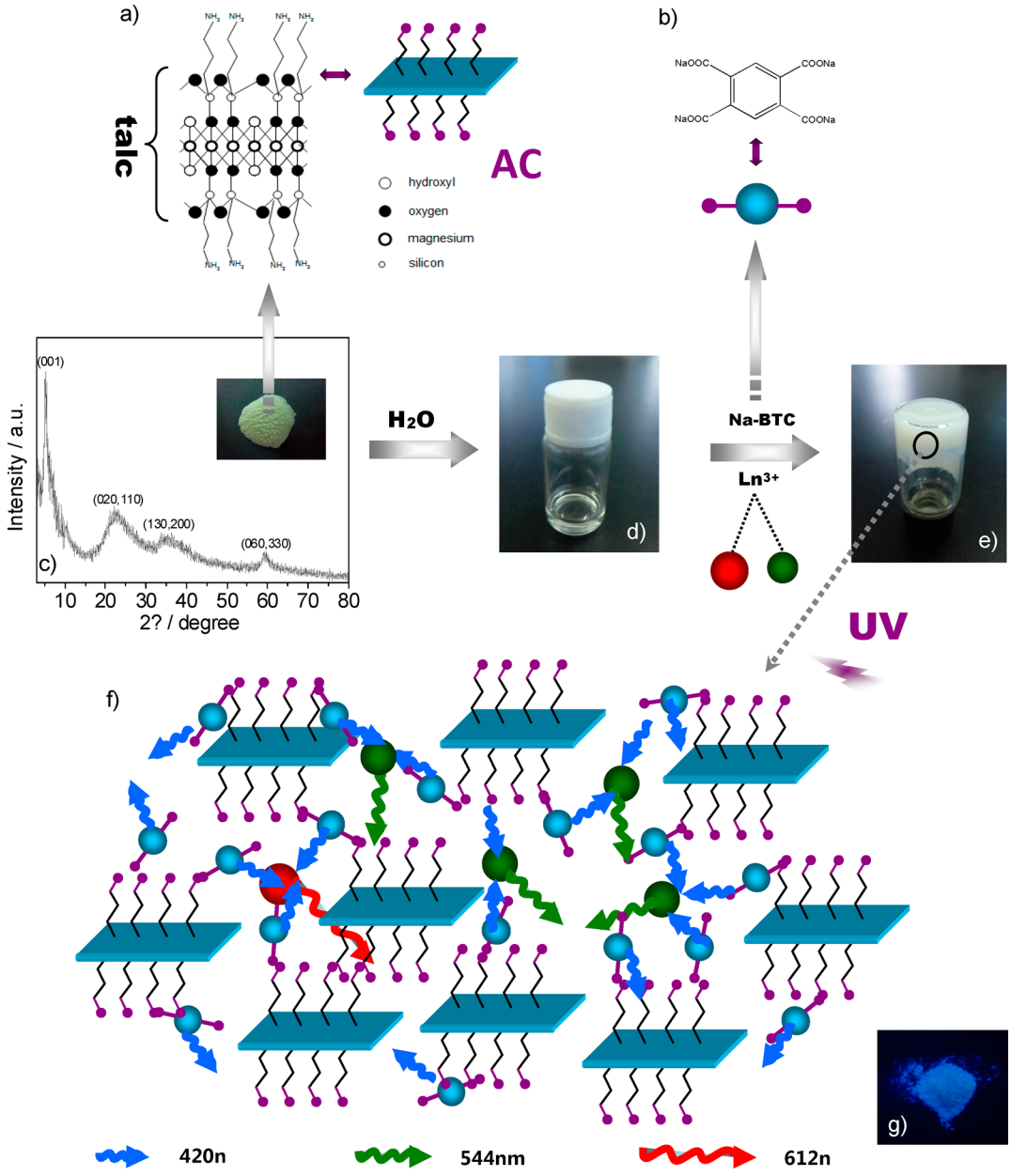

[a]a) a single AC unit; b) Na-BTC; c) digital photo and XRD pattern of AC, $d_{(001)}$ = 1.64 nm (2θ = 5.3°) exhibits a regular layered-structure thickness of the talc-like phyllosilicate, $d_{(020,\ 110)}$ = 0.407 nm (2θ = 22°), $d_{(130,\ 200)}$ = 0.256 nm (2θ = 35°), and $d_{(060,\ 330)}$ = 0.156 nm (2θ = 59°) reveals the formation of the 2:1 trioctahedral smectite structure;[7] d) AC aqueous solution; e) AC-BTC-Ln (hydrogel), with approximate molar ratio of AC: Na-BTC = 13:7 and Na-BTC: Ln^{3+} = 3:4; f) schematic representation of the luminescent materials consist of AC, Na-BTC and $LnCl_3$, under UV light illumination; g) image of the dehydrated fine powder of AC-BTC (254 nm UV illumination).

conditions such as exclusion of water molecules, reduced pressure, and time-consuming. It is therefore highly desirable to develop luminescent materials of tunable emissions and white lighting through a simple, environmentally benign, low-cost, and less time-consuming procedure.

Herein, we report a fascinating multicolored photoluminescent and white-light-emitting hybrid composite by simple supramolecular coassembly of organoclay, sensitizer as well as Ln^{3+} in aqueous medium at room temperature. The preparation of the luminescent composite shown in Scheme 1 is based on the noncovalent ionic assembly between the anionic organic sensitizer and the cationic aminoclay (AC) in water. The aminoclay, a kind of layered magnesium organosilicate which is talc-like and has an approximate composition of $R_8Si_8Mg_6O_{16}(OH)_4$ where R− is aminopropyl ($NH_2CH_2CH_2CH_2-$),[7−9] was selected as the scaffold for the organization of Ln^{3+} and the organic sensitizers because the protonation of the amino groups in water can guarantee the complete exfoliation of clay layers and can interact electrostatically with the negatively charged sensitizers (Scheme 1a).[11] The XRD pattern (Scheme 1c) reveals a disordered structure of the as-synthesized aminoclay. Sodium 1,2,4,5-benzenetetracarboxylate (Scheme 1b) which we denote as Na-BTC was employed as the anionic organic sensitizer for Ln^{3+} ions. The negatively charged carboxylate groups are expected to interact electrostatically with the positively charged organoclay and Ln^{3+}

ions in water to result in noncovalent hybrid composites. When Na-BTC and AC aqueous solution are mixed in an appropriate molar ratio, a hydrogel is formed. Dehydration of the obtained hydrogel at 80 °C in air for several hours yields the final material named AC-BTC, which has blue fluorescence under UV lamp illumination (Scheme 1g). Luminescent materials with tunable emission colors are easily obtained by mixing the aqueous solution of Na-BTC, AC, and $LnCl_3$ (Ln^{3+} = Eu^{3+}, Tb^{3+}, or Eu^{3+} and Tb^{3+} in different molar ratios) which we denoted as AC-BTC-Eu, AC-BTC-Tb, and AC-BTC-Eu_xTb_y, respectively, where the molar ratio of Eu^{3+} and Tb^{3+} is represent by x/y (Scheme 1f and Figure 1A). Furthermore,

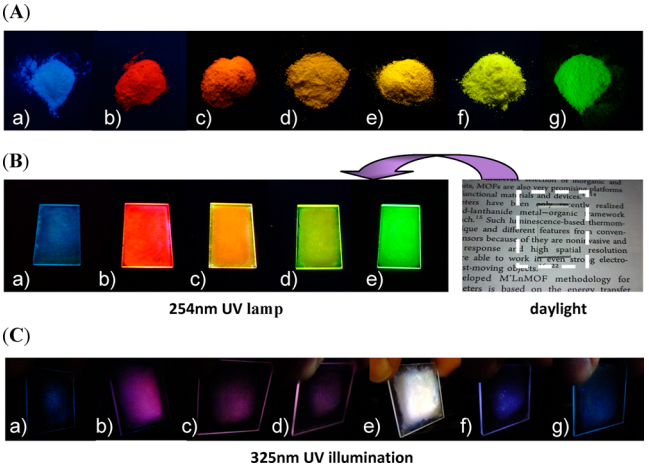

Figure 1. (**A**)-Images of luminescent materials with tunable emission colors under 254 nm UV lamp illumination: a) AC-BTC; b) AC-BTC-Eu; c) AC-BTC-Eu_1Tb_2; d) AC-BTC-Eu_1Tb_4; e) AC-BTC-Eu_1Tb_7; f) AC-BTC-Eu_1Tb_{19}; g) AC-BTC-Tb. (**B**)-Images of transparent and luminescent films on quartz substrate: a) AC-BTC; b) AC-BTC-Eu; c) AC-BTC-Eu_1Tb_2; d) AC-BTC-Eu_1Tb_7; e) AC-BTC-Tb, with excitation wavelength of 254 nm. (**C**)-Images of the films on quartz substrate: a) AC-BTC; b) AC-BTC-Eu; c) AC-BTC-Eu_1Tb_2; d) AC-BTC-Eu_1Tb_4; e) AC-BTC-Eu_1Tb_7; f) AC-BTC-Eu_1Tb_{19}; g) AC-BTC-Tb, under 325 nm UV light illumination.

transparent and luminescent films exhibiting various emission colors can be facilely achieved by drop-casting of the hydrogels onto quartz substrate (Figure 1B and 1C). Remarkably, the materials and their corresponding transparent films show various emission colors as evidenced from the CIE (Commission Internationale de L'Eclairage) coordinates under proper concentration of the various components, appropriate excitation wavelength, and temperature.

2. RESULTS AND DISCUSSION

The excitation spectrum of hybrid composite AC-BTC-Eu (see Figure S1a, Supporting Information) shows a broad band between 230 and 340 nm attributed to the absorption of BTC and several sharp lines from 350 to 500 nm assigned to intra4f^6 transitions of Eu^{3+} between $^7F_0$ and the $^5D_4$, $^5G_2$, $^5L_6$, and $^5D_{3-1}$ levels. The emission spectrum (Figure 2a) excited at 300 nm exhibits five sharp bands at 579, 592, 612, 650, and 699 nm, ascribed to the $^5D_0 \rightarrow {}^7F_J$ (J = 0–4) transitions of Eu^{3+}. It is dominated by the $^5D_0 \rightarrow {}^7F_2$ band at 612 nm, which is responsible for the red emission color shown in Figure 1A, b. The excitation spectrum of hybrid composite AC-BTC-Tb (Figure S1b, Supporting Information) is composed of a broad band peaking at 260 and 300 nm ascribed to BTC and the f-f

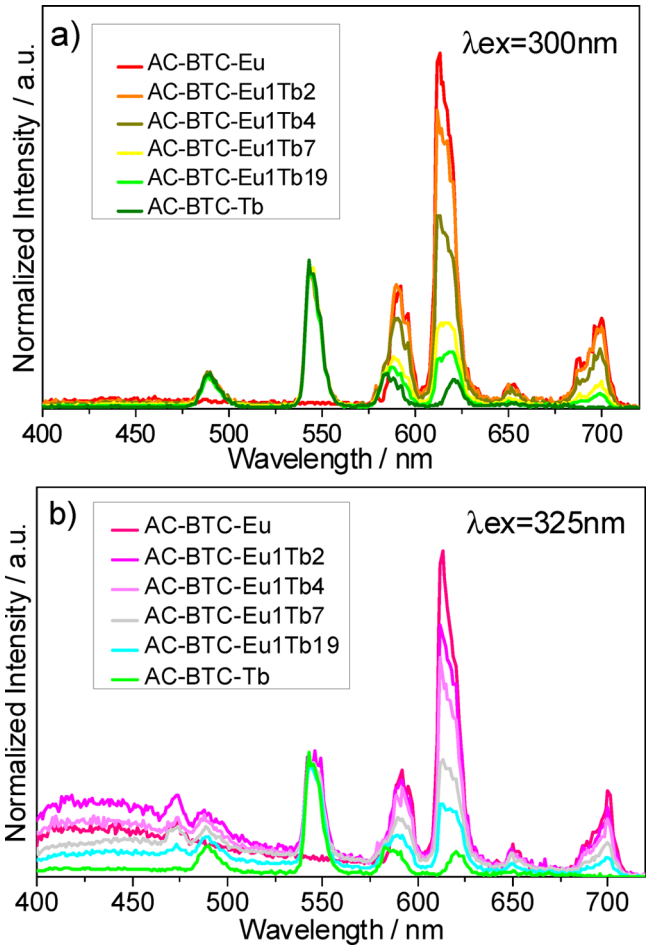

Figure 2. Emission spectra of the luminescent materials excited by a wavelength of 300 nm (a) and 325 nm (b). The spectra are normalized according to the peaking intensity of the $^5D_4 \rightarrow {}^7F_5$ transition of Tb^{3+}.

lines assigned to Tb^{3+}. Excitation at 300 nm results in line-shaped emission bands (Figure 2a), which are assigned to the transitions of Tb^{3+} from the $^5D_4$ level to the ^7F_J levels (J = 6, 5, 4, 3) at 490, 544, 584, and 620 nm, respectively. The $^5D_4 \rightarrow {}^7F_5$ transition dominates the whole emission spectrum and is responsible for the bright green emission color shown in Figure 1A, g. We also measured the lifetime of the $^5D_0$ state (Eu^{3+} in AC-BTC-Eu) and the $^5D_4$ state (Tb^{3+} in AC-BTC-Tb), which is 0.37 and 1.00 ms, respectively (see Figure S2, Supporting Information). The excitation spectra of the Eu^{3+} and Tb^{3+} codoping hybrid composites (named as AC-BTC-Eu_xTb_y, Figure S1c, Supporting Information) are fundamentally identical to that of AC-BTC-Eu, except for the less intense f-f transition lines of Eu^{3+} in materials. The emission colors of AC-BTC-Eu_xTb_y can be simply tuned by varying the molar ratio of Eu^{3+} to Tb^{3+} as revealed in Figure 1A and Table S1. The emission spectra after excitation at 300 nm shown in Figure 2a display characteristic sharp bands at 488, 543, 582, and 620 nm, attributed to the f-f transitions of Tb^{3+} ($^5D_4 \rightarrow {}^7F_J$, J = 6, 5, 4, 3) with $^5D_4 \rightarrow {}^7F_5$ transition (green emission) as the dominant feature. The bands at 580, 595, 612, 652, and 702 nm attributed to Eu^{3+}, namely the $^5D_0 \rightarrow {}^7F_J$ (J = 0, 1, 2, 3, 4) transitions with $^5D_0 \rightarrow {}^7F_2$ transition (red emission) as the dominant feature. The emission color of AC-BTC-Eu_xTb_y is highly dependent on the molar ratio of Eu^{3+} and Tb^{3+}. When changing this molar

dx.doi.org/10.1021/am5028555 | ACS Appl. Mater. Interfaces 2014, 6, 12915–12921

ratio, we observe that the red component of the emission decreases drastically upon increasing the Tb^{3+} concentration. The colors obtained thus varied from red to green through yellow as shown in Figure 1A and Figure 3.

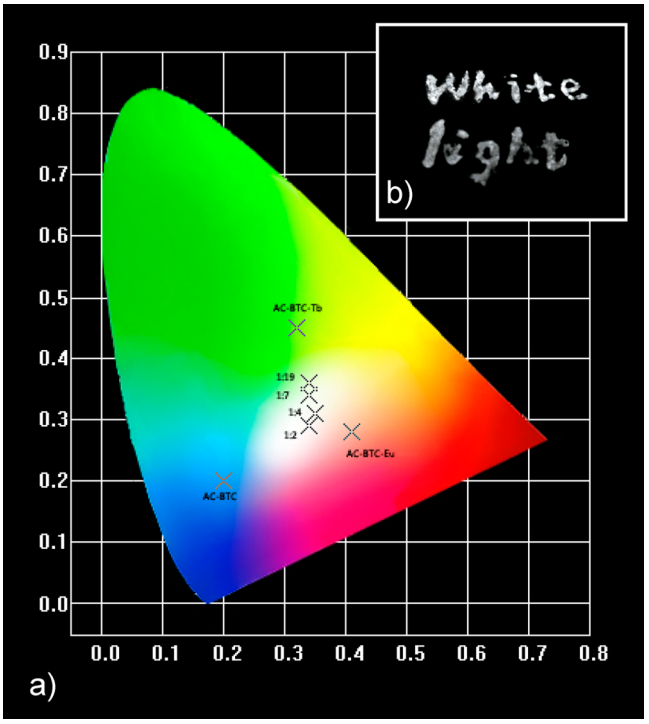

Figure 3. a) CIE 1931 chromaticity diagram within the coordinates of the luminescent materials under 325 nm UV illumination; b) image of AC-BTC-Eu_1Tb_7 hydrogel written as "White light" under 365 nm UV lamp illumination.

Furthermore, the emission colors can also be tuned by changing the excitation wavelength. When the excitation wavelength was increased to 325 nm, the emission spectra of the hybrid materials show a broad band in the blue region, in addition to the green emission from Tb^{3+} ion and red emission from Eu^{3+} as shown in Figure 2b. The blue component with maximum at 420 nm in the blue region can be attributed to the emission of the organic sensitizer. This indicates that the energy transfer from ligand to Ln^{3+} ions is not very efficient when excited at 325 nm. Actually, excitation wavelength-dependence energy transfer is usually observed.[6,27] The persistence of the blue emission in the presence of Eu^{3+} and Tb^{3+} affords the white emission in the hybrid composites where the molar concentration of Eu^{3+} to Tb^{3+} is 1:7 (AC-BTC-Eu_1Tb_7) as evidenced by the CIE coordinate of (0.34, 0.34) shown in Figure 3 and Table S1, which is nearly close to the designed coordinate for the ideal white light (0.33, 0.33).

In addition, the luminescent behavior of the hybrid materials can also be tuned by temperature variation. The temperature-dependent luminescence spectra of AC-BTC-Eu, AC-BTC-Tb, and AC-BTC-Eu_1Tb_7 (78 K to 288 K, ΔT = 30 K) are shown in Figure 4a-c, respectively. The $^5D_0 \rightarrow {}^7F_2$ transition (612 nm) of AC-BTC-Eu and the $^5D_4 \rightarrow {}^7F_5$ transition (543 nm) of AC-BTC-Tb have the similar temperature-dependent luminescent behavior (Figure 4d); both the emission intensity of Eu^{3+} and Tb^{3+} in AC-BTC-Eu and AC-BTC-Tb have no obvious variation, while the temperature varies from 78 K to 258 K and then suddenly decreases really fast by 1.19% per K for AC-BTC-Eu and 0.74% per K for AC-BTC-Tb on increasing temperature from 258 to 288 K, respectively, which is larger than the value reported recently for the lanthanide metal organic framework materials.[30] The decrease in emission intensity upon increasing temperature can be ascribed to the thermal activation of nonradiative-decay channels.[31,32] How-

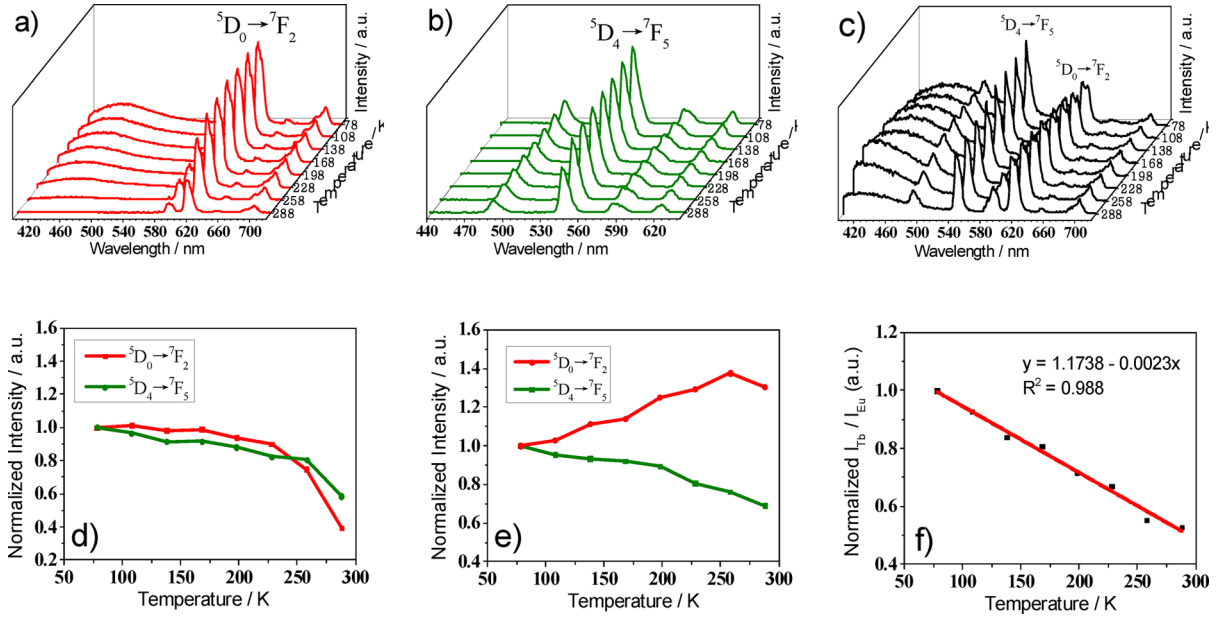

Figure 4. Temperature-dependent emission spectra of a) AC-BTC-Eu (excited at 300 nm), b) AC-BTC-Tb (excited at 300 nm), and c) AC-BTC-Eu_1Tb_7 (excited at 325 nm); d) temperature dependence of normalized intensity of the $^5D_0 \rightarrow {}^7F_2$ transition (612 nm) for AC-BTC-Eu (red curve) and $^5D_4 \rightarrow {}^7F_5$ transition (543 nm) for AC-BTC-Tb (green curve); e) temperature dependence of normalized intensity of the $^5D_0 \rightarrow {}^7F_2$ (red curve) and $^5D_4 \rightarrow {}^7F_5$ (green curve) transitions for AC-BTC-Eu_1Tb_7 (78 K to 288 K, ΔT = 30 K); f) temperature dependence of the normalized intensity ratio of Tb^{3+} to Eu^{3+} for AC-BTC-Eu_1Tb_7 from 78 K to 288 K (excited at 325 nm). The curve was fitted through a linear function (I_{Tb}/I_{Eu} = 1.1738−0.0023T, T = temperature, R^2 = 0.988).

dx.doi.org/10.1021/am5028555 | ACS Appl. Mater. Interfaces 2014, 6, 12915−12921

Figure 5. Images of a) commercial available UV-LED cell (λ_{em} = 365−370 nm, 3.2−3.8 V, 20 mA); b) UV-LED coated with the AC-BTC-Eu_1Tb_7 hydrogel, which has a bright white light when the LED is on in image c.

ever, unexpectedly, the AC-BTC-Eu_1Tb_7 exhibits a conspicuously different temperature-dependent luminescent behavior from those of AC-BTC-Eu and AC-BTC-Tb. The emission intensity of the $^5D_0 \rightarrow {}^7F_2$ transition (612 nm) increases gradually from 78 K to 258 K and then decreases, while that of the $^5D_4 \rightarrow {}^7F_5$ transition (543 nm) decreases continuously with the increase in temperature (Figure 4e). This is possibly due to the partial energy transfer from Tb^{3+} to Eu^{3+} in AC-BTC-Eu_1Tb_7, and the energy transform efficiency from Tb^{3+} to Eu^{3+} in AC-BTC-Eu_1Tb_7 ($\eta_{Tb\rightarrow Eu}$) can be estimated according to eq 1 as follows[30]

$$\eta_{Tb\rightarrow Eu} = 1 - \tau_1/\tau_0 \quad (1)$$

where τ_0 and τ_1 are the lifetime of the $^5D_4$ state in AC-BTC-Tb and AC-BTC-Eu_1Tb_7, respectively. The τ_0 is 1.00 ms, as obtained previously. Therefore, we measured the lifetimes of the $^5D_4$ state in AC-BTC-Eu_1Tb_7 (78 K to 288 K, excited at 325 nm) and exhibited them in Table S2, and the $\eta_{Tb\rightarrow Eu}$ curve of AC-BTC-Eu_1Tb_7 with the variation of temperature was shown in Figure S3 (see the Supporting Information). Apparently, the $\eta_{Tb\rightarrow Eu}$ increases steadily with the increase of temperature. This strongly confirmed that the energy transfer from Tb^{3+} to Eu^{3+} in AC-BTC-Eu_1Tb_7 occurs, and the efficiency of which is also temperature-dependent.

Since the AC-BTC-Eu_1Tb_7 shows different temperature-dependent luminescent behavior of $^5D_0 \rightarrow {}^7F_2$ and $^5D_4 \rightarrow {}^7F_5$ transitions, it is potentially available for designing a self-referencing luminescent thermometer. Therefore, we studied the temperature-dependent emission intensity ratio of $^5D_4 \rightarrow {}^7F_5$ transition to $^5D_0 \rightarrow {}^7F_2$ transition of AC-BTC-Eu_1Tb_7 (I_{Tb}/I_{Eu}), as shown in Figure 4f. Remarkably, the I_{Tb}/I_{Eu} can be linearly related to temperature by the following equation from 78 K to 288 K

$$T = 510.35 - 434.78 I_{Tb}/I_{Eu}\ (K) \quad (2)$$

which is the equivalent transformation of the equation I_{Tb}/I_{Eu} = 1.1738−0.0023T. This indicates that the AC-BTC-Eu_1Tb_7 is a brilliant luminescent thermometer in the temperature range from 78 K to 288 K, which does not require any extra calibration of the emission intensity. Although several luminescent thermometers based on lanthanide have been reported,[32−38] self-referencing luminescent thermometers are rarely reported[30,39] despite obvious advantages compared with other types of solid luminescent thermometers. The AC-BTC-Eu_1Tb_7 can also emit different colors from cyan to white when the temperature changes (see Figure S4, Supporting Information), and the CIE coordinates of these emission colors are shown in Table S3. When the temperature increases to 288 K (15 °C), the CIE coordinate of AC-BTC-Eu_1Tb_7 is (0.34, 0.31), which is very close to the (0.34, 0.34) that was measured at room temperature (about 25 to 30 °C), indicating that the AC-BTC-Eu_1Tb_7 is thermostable. Moreover, the temperature-dependent emission spectra of which is reversible when the temperature varies between the boiling point of nitrogen (77 K) and room temperature.

Since the success in preparing thin films constitutes the prerequisite for a luminescent material to be used in device fabrication, we therefore have prepared transparent films of the hybrid materials, which were easily prepared by drop-casting the hydrogels onto quartz substrate. The emissions of the transparent films are tuned through altering the molar ratio of Eu^{3+} to Tb^{3+}. The emission spectra of the films shown in Figure S5 (Supporting Information) are similar to those seen in Figure 2. Excitation at 300 nm results in red emissions for Eu^{3+}, green emissions for Tb^{3+}, and the mixture emissions for Eu^{3+} and Tb^{3+} codoping thin films. An increased green emission can be observed when decreasing the molar ratio of Eu^{3+} and Tb^{3+}, whereas the red emission decreases remarkably, the emission colors of the films thus can be systematically tuned, as shown in Figure 1B and Table S4. Similarly, excitation at 325 nm results in emission spectra which are composed of the blue component (sensitizer), the red component (Eu^{3+}), and the green component (Tb^{3+}). When the molar ratio of Eu^{3+} and Tb^{3+} is 1:7, the luminescent film shows a white light with a CIE coordinate of (0.32, 0.28). In addition to being casted on the flat substrate to get luminescent films, the gels can be easily coated on round shaped objectives like an UV-LED cell and then a bright white light is achieved (Figure 5). Therefore, we can conclude here that the emission colors of the luminescent films can be similarly tuned by changing the molar ratio of Eu^{3+} and Tb^{3+} as well as by changing the excitation wavelength.

3. CONCLUSION

In summary, a novel kind of solution processable luminescent materials based on organoclay, organic sensitizer, and Ln^{3+} have been successfully achieved through a simple, environmentally friendly, low-cost, and less time-consuming procedure. Various emission colors including white light with good color purity can be achieved by changing the molar ratio of Eu^{3+} and Tb^{3+} and altering the excitation wavelength as well as varying the temperature. Interestingly, the hybrid material with a Eu^{3+} to Tb^{3+} molar ratio of 1:7 exhibits a brilliant temperature-dependent luminescent behavior from 78 K to 288 K, enabling it to be a candidate for self-referencing luminescent thermometers. The solution processability of the novel luminescent hybrids has been well demonstrated by the easy fabrication of transparent films and painting on round-shaped objectives such as UV-LED cell from aqueous medium, which affords them ideal candidates for fabricating devices used as display and lighting in an environmentally friendly way.

4. EXPERIMENTAL SECTION

4.1. Materials. 3-Aminopropyltriethoxysilane (APTES, Aldrich), $MgCl_2{\cdot}6H_2O$ (CP), pyromellitic dianhydride (PMDA, AR), Eu_2O_3 (99.99%), and Tb_4O_7 (99.99%) were used as received. Na-BTC aqueous solution (0.07M) was obtained by dissolving PMDA into 0.3 M NaOH aqueous solution. $EuCl_3{\cdot}6H_2O$ and $TbCl_3{\cdot}6H_2O$ were obtained by dissolving Eu_2O_3 and Tb_4O_7 into concentrated hydrochloric acid (37%), respectively.

4.2. Synthesis of Aminoclay (AC). AC was prepared by the following method: The APTES (2.46 g, 11.1 mmol) was added dropwise to a stirred solution of $MgCl_2{\cdot}6H_2O$ (1.68 g, 8.3 mmol) in absolute alcohol (50 mL) and the white emulsion stirred for 24 h at room temperature (20−25 °C). The precipitated white solid was isolated by centrifugation (10000 rpm, 6 min), washed with absolute alcohol (2 × 50 mL), and dried at 80 °C in air for several hours. Afterward, the product was finely ground into a white to light yellow powder.

4.3. Synthesis of the AC-BTC-Ln. AC was dissolved in an appropriate amount of double distilled water (about 15 wt %), then we added Na-BTC aqueous solution and 0.1 mol/L $LnCl_3{\cdot}6H_2O$ aqueous solution (Ln^{3+} = Eu^{3+}, Tb^{3+}, or Eu^{3+} and Tb^{3+} in different molar ratio) quickly to the AC aqueous solution with an approximate molar ratio of AC:Na-BTC = 13:7 and Na-BTC:Ln^{3+} = 3:4, and a white hydrogel was formed. Finally, we dried the hydrogel at 80 °C in air for several hours and ground it into a fine powder, and the hybrid luminescent materials (AC-BTC-Eu, AC-BTC-Eu_1Tb_2, AC-BTC-Eu_1Tb_4, AC-BTC-Eu_1Tb_7, AC-BTC-Eu_1Tb_{19}, and AC-BTC-Tb) were successfully synthesized. The luminescent and transparent films were also obtained by simply drop-casting the materials onto quartz substrate.

4.4. Characterization. The X-ray diffraction (XRD) measurements were carried out on powdered samples by using a Bruker D8 diffractometer (40 mA, 40 kV) with monochromated Cu−Kα1 radiation (λ = 0.15405 nm).

The solid-state luminescence spectra and the lifetimes were measured on an Edinburgh Instrument FS920P spectrometer, with a 450 W xenon lamp as the steady-state excitation source, a double excitation monochromator (1800 lines mm^{-1}), an emission monochromator (600 lines mm^{-1}), and a semiconductor cooled Hamamatsu RMP928 photomultiplier tube. Powder samples and films on quartz substrate were directly put in the chamber of the instrument, for the phtotophysical measurements. A microsecond flash lamp (pulse length: 2 μs) was used as the excitation source for the lifetime measurements. Photons were collected up to 10 ms until a maximum of 10^4 counts. Decay curves were fitted according to the single-exponential function ($I = I_0 + A * \exp[-(t-t_0)/\tau]$). The OptistatDN2 liquid nitrogen cryostat was used for the measurement of the temperature-dependent luminescence spectra.

ASSOCIATED CONTENT

Supporting Information

Excitation spectra of AC-BTC-Eu, AC-BTC-Tb, and AC-BTC-Eu_xTb_y, decay curves of the $^5D_0$ state of Eu^{3+} in AC-BTC-Eu and the $^5D_4$ state of Tb^{3+} in AC-BTC-Tb, $\eta_{Tb\rightarrow Eu}$ curve of AC-BTC-Eu_1Tb_7, CIE 1931 chromaticity diagram within the coordinates of AC-BTC-Eu_1Tb_7 at different temperatures, emission spectra of the transparent films, CIE 1931 chromaticity diagram within the coordinates of the transparent films on quartz and the picture of AC-BTC-Eu_1Tb_7 transparent film, CIE coordinates of the luminescent materials, lifetime of the $^5D_4$ state in AC-BTC-Eu_1Tb_7 with the variation of temperature, CIE coordinates of the AC-BTC-Eu_1Tb_7 from 78 K to 288 K and CIE coordinates of the transparent films. This material is available free of charge via the Internet at http://pubs.acs.org.

AUTHOR INFORMATION

Corresponding Author

*Phone: 86-22-60203674. Fax: 86-22-60204294. E-mail: lihuanrong@hebut.edu.cn.

Notes

The authors declare no competing financial interest.

ACKNOWLEDGMENTS

Financial support by the National Key Basic Research Program (2012CB626804), the National Natural Science Foundation of China (20901022, 21171046, 21271060, and 21236001), the Tianjin Natural Science Foundation (13JCYBJC18400), the Natural Science Foundation of Hebei Province (No. B2013202243), the Program for Changjiang Scholars and Innovative Research Team in University (PCSIRT, IRT1059), and Educational Committee of Hebei Province (2011141, LJRC021) is gratefully acknowledged.

REFERENCES

(1) Santhosh Babu, S.; Aimi, J.; Ozawa, H.; Shirahata, N.; Saeki, A.; Seki, S.; Ajayaghosh, A.; Möhwald, H.; Nakanishi, T. Solvent-Free Luminescent Organic Liquids. *Angew. Chem., Int. Ed.* **2012**, *51*, 3391−3395.

(2) Abbel, R.; Grenier, C.; Pouderoijen, M. J.; Stouwdam, J. W.; Leclère, P. E. L. G; Sijbesma, R. P.; Meijer, E. W.; Schenning, A. P. H. J. White-Light Emitting Hydrogen-Bonded Supramolecular Copolymers Based on π-Conjugated Oligomers. *J. Am. Chem. Soc.* **2008**, *131*, 833−843.

(3) Kamtekar, K. T.; Monkman, A. P.; Bryce, M. R. Recent Advances in White Organic Light-Emitting Materials and Devices (WOLEDs). *Adv. Mater.* **2010**, *22*, 572−582.

(4) Farinola, G. M.; Ragni, R. Electroluminescent Materials for White Organic Light Emitting Diodes. *Chem. Soc. Rev.* **2011**, *40*, 3467−3482.

(5) Ajayaghosh, A.; Praveen, V. K.; Vijayakumar, C. Organogels as Scaffolds for Excitation Energy Transfer and Light Harvesting. *Chem. Soc. Rev.* **2008**, *37*, 109−122.

(6) Wada, Y.; Sato, M.; Tsukahara, Y. Fine Control of Red-Green-Blue Photoluminescence in Zeolites Incorporated with Rare-Earth Ions and A Photosensitizer. *Angew. Chem., Int. Ed.* **2006**, *45*, 1925−1928.

(7) Lee, Y. C.; Lee, K.; Hwang, Y.; Andersen, H. R.; Kim, B.; Lee, S. Y.; Choi, M. H.; Park, J. Y.; Han, Y. K.; Oh, Y. K.; Huh, Y. S. Aminoclay-templated Nanoscale Zero-valent Iron (nZVI) Synthesis for Efficient Harvesting of Oleaginous Microalga, Chlorellasp. KR-1. *RSC Adv.* **2014**, *4*, 4122−4127.

(8) Hwang, Y.; Lee, Y. C.; Mines, P. D.; Huh, Y. S.; Andersen, H. R. Nanoscale Zero-valent Iron (nZVI) Synthesis in A Mg-aminoclay Solution Exhibits Increased Stability and Reactivity for Reductive Decontamination. *Appl. Catal., B* **2014**, *147*, 748−755.

(9) Lee, Y. C.; Lee, H. U.; Lee, K.; Kim, B.; Lee, S. Y.; Choi, M. H.; Farooq, W.; Choi, J. S.; Park, J. Y.; Lee, J.; Oh, Y. K.; Huh, Y. S. Aminoclay-conjugated TiO_2 Synthesis for Simultaneous Harvesting and Wet-disruption of Oleaginous *Chlorella* sp. *Chem. Eng. J.* **2014**, *245*, 143−149.

(10) Rao, K. V.; Datta, K. K. R.; Eswaramoorthy, M.; George, S. J. Light-Harvesting Hybrid Assemblies. *Chem.—Eur. J.* **2012**, *18*, 2184−2194.

(11) Rao, K. V.; Datta, K. K. R.; Eswaramoorthy, M.; George, S. J. Highly Pure Solid-State White-Light Emission from Solution-Processable Soft-Hybrids. *Adv. Mater.* **2013**, *25*, 1713−1718.

(12) Rao, K. V.; Datta, K. K. R.; Eswaramoorthy, M.; George, S. J. Light-Harvesting Hybrid Hydrogels: Energy-Transfer-Induced Amplified Fluorescence in Noncovalently Assembled Chromophore-Organoclay Composites. *Angew. Chem., Int. Ed.* **2011**, *50*, 1179−1184.

(13) Cuan, J.; Yan, B. Cool-White Light Emitting Hybrid Materials of A Resin-Mesoporous Silica Composite Matrix Encapsulating Euro-

pium Polyoxometalates through An Ionic Liquid Linker. *RSC Adv.* **2013**, *3*, 20077−20084.
(14) Narayana, Y. S. L. V.; Basak, S.; Baumgarten, M.; Müllen, K.; Chandrasekar, R. White-Emitting Conjugated Polymer/Inorganic Hybrid Spheres: Phenylethynyl and 2,6-Bis(pyrazolyl)pyridine Co-polymer Coordinated to $Eu(tta)_3$. *Adv. Funct. Mater.* **2013**, *23*, 5875−5880.
(15) Zhang, H.; Shan, X.; Zhou, L.; Lin, P.; Li, R.; Ma, E.; Guo, X.; Du, S. Full-Colour Fluorescent Materials Based on Mixed-Lanthanide-(iii) Metal-Organic Complexes with High-Efficiency White Light Emission. *J. Mater. Chem. C* **2013**, *1*, 888−891.
(16) Dai, Q.; Foley, M. E.; Breshike, C. J.; Lita, A.; Strouse, G. F. Ligand-Passivated $Eu:Y_2O_3$ Nanocrystals as A Phosphor for White Light Emitting Diodes. *J. Am. Chem. Soc.* **2011**, *133*, 15475−15486.
(17) Carlos, L. D.; Ferreira, R. A. S.; Bermudez, V. D. Z.; Ribeiro, S. J. L. Lanthanide-Containing Light-Emitting Organic-Inorganic Hybrids: A Bet on the Future. *Adv. Mater.* **2009**, *21*, 509−534.
(18) Binnemans, K. Lanthanide-Based Luminescent Hybrid Materials. *Chem. Rev.* **2009**, *109*, 4283−4374.
(19) Feng, J.; Zhang, H. Hybrid Materials Based on Lanthanide Organic Complexes: A Review. *Chem. Soc. Rev.* **2013**, *42*, 387−410.
(20) Coppo, P.; Duati, M.; Kozhevnikov, V. N.; Hofstraat, J. W.; De Cola, L. White-Light Emission from An Assembly Comprising Luminescent Iridium and Europium Complexes. *Angew. Chem., Int. Ed.* **2005**, *44*, 1806−1810.
(21) He, G.; Guo, D.; He, C.; Zhang, X.; Zhao, X.; Duan, C. A Color-Tunable Europium Complex Emitting Three Primary Colors and White Light. *Angew. Chem., Int. Ed.* **2009**, *48*, 6132−6135.
(22) Eliseeva, S. V.; Bunzli, J.-C.G. Lanthanide Luminescence for Functional Materials and Bio-sciences. *Chem. Soc. Rev.* **2010**, *39*, 189−227.
(23) Yan, B. Recent Progress in Photofunctional Lanthanide Hybrid Materials. *RSC Adv.* **2012**, *2*, 9304−9324.
(24) Li, P.; Wang, Y.; Li, H.; Calzaferri, G. Luminescence Enhancement after Adding Stoppers to Europium(III) Nanozeolite L. *Angew. Chem., Int. Ed.* **2014**, *53*, 2904−2909.
(25) Wang, Y.; Li, H.; Gu, L.; Gan, Q.; Li, Y.; Calzaferri, G. Thermally Stable Luminescent Lanthanide Complexes in Zeolite L. *Microporous Mesoporous Mater.* **2009**, *121*, 1−6.
(26) Ding, Y.; Wang, Y.; Li, H.; Duan, Z.; Zhang, H.; Zheng, Y. Photostable and Efficient Red-emitters Based on Zeolite L Crystals. *J. Mater. Chem.* **2011**, *21*, 14755−14759.
(27) Zhao, D.; Seo, S. J.; Bae, B. S. Full-Color Mesophase Silicate Thin Film Phosphors Incorporated with Rare Earth Ions and Photosensitizers. *Adv. Mater.* **2007**, *19*, 3473−3479.
(28) Heer, S.; Kömpe, K.; Güdel, H. U.; Haase, M. Highly Efficient Multicolour Upconversion Emission in Transparent Colloids of Lanthanide-Doped $NaYF_4$ Nanocrystals. *Adv. Mater.* **2004**, *16*, 2102−2105.
(29) Fu, L.; Liu, Z.; Liu, Y.; Han, B.; Wang, J.; Hu, P.; Cao, L.; Zhu, D. Ga_2O_3 Nanoribbons-Eu_2O_3 Multisheaths Heterostructure and Energy Transfer. *J. Phys. Chem. B* **2004**, *108*, 13074−13078.
(30) Rao, X.; Song, T.; Gao, J.; Cui, Y.; Yang, Y.; Wu, C.; Chen, B.; Qian, G. A Highly Sensitive Mixed Lanthanide Metal-Organic Framework Self-Calibrated Luminescent Thermometer. *J. Am. Chem. Soc.* **2013**, *135*, 15559−15564.
(31) Bhaumik, M. L. Quenching and Temperature Dependence of Fluorescence in Rare-Earth Chelates. *J. Chem. Phys.* **1964**, *40*, 3711−3715.
(32) Peng, H.; Stich, M. I. J.; Yu, J.; Sun, L.-N.; Fischer, L. H.; Wolfbeis, O. S. Luminescent Europium(III) Nanoparticles for Sensing and Imaging of Temperature in the Physiological Range. *Adv. Mater.* **2010**, *22*, 716−719.
(33) Brites, C. D. S.; Lima, P. P.; Silva, N. J. O.; Millán, A.; Amaral, V. S.; Palacio, F.; Carlos, L. D. A Luminescent Molecular Thermometer for Long-Term Absolute Temperature Measurements at the Nanoscale. *Adv. Mater.* **2010**, *22*, 4499−4504.
(34) Vetrone, F.; Naccache, R.; Zamarrón, A.; Juarranz de la Fuente, A.; Sanz-Rodríguez, F.; Martinez Maestro, L.; Martín Rodriguez, E.; Jaque, D.; García Solé, J.; Capobianco, J. A. Temperature Sensing Using Fluorescent Nanothermometers. *ACS Nano* **2010**, *4*, 3254−3258.
(35) Sun, L.-N.; Yu, J.; Peng, H.; Zhang, J. Z.; Shi, L.-Y.; Wolfbeis, O. S. Temperature-Sensitive Luminescent Nanoparticles and Films Based on A Terbium (III) Complex Probe. *J. Phys. Chem. C* **2010**, *114*, 12642−12648.
(36) Yu, J.; Sun, L.; Peng, H.; Stich, M. I. J. Luminescent Terbium and Europium Probes for Lifetime Based Sensing of Temperature Between 0 and 70 °C. *J. Mater. Chem.* **2010**, *20*, 6975−6981.
(37) Wang, X.-d.; Wolfbeis, O. S.; Meier, R. J. Luminescent Probes and Sensors for Temperature. *Chem. Soc. Rev.* **2013**, *42*, 7834−7869.
(38) Brites, C. D. S.; Lima, P. P.; Silva, N. J. O.; Millan, A.; Amaral, V. S.; Palacio, F.; Carlos, L. D. Thermometry at the Nanoscale. *Nanoscale* **2012**, *4*, 4799−4829.
(39) Cui, Y.; Xu, H.; Yue, Y.; Guo, Z.; Chen, Z.; Gao, J.; Yang, Y.; Qian, G.; Chen, B. A Luminescent Mixed-Lanthanide Metal-Organic Framework Thermometer. *J. Am. Chem. Soc.* **2012**, *134*, 3979−3982.